Materials Research Proceedings **2** (2016) 609-614 doi: http://dx.doi.org/10.21741/9781945291173-103

Dislocation Density of GlidCop with Compressive Strain applied at High Temperature

Mutsumi Sano[1*], Sunao Takahashi[1], Atsuo Watanabe[1], Ayumi Shiro[2], Takahisa Shobu[3]

[1]JASRI, 1-1-1 Kouto Sayo-cho, Sayo-gun, Hyogo 679-5198, Japan

[2]QST Quantum Beam Research Directorate 1-1-1 Kouto Sayo-cho, Sayo-gun, Hyogo 679-5148, Japan

[3]JAEA Materials Sciences Research Center, 1-1-1 Kouto Sayo-cho, Sayo-gun, Hyogo 679-5148, Japan

* musano@spring8.or.jp

Keywords: Dislocation Density, GlidCop, Plastic Strain, Profile Analysis

Abstract. Dislocation densities of GlidCop with compressive strain applied at high temperature were examined by X-ray line profile analyses with synchrotron radiation. In order to evaluate the dislocation density, we applied the modified Williamson-Hall and modified Warren-Averbach method. The dislocation densities of GlidCop with compressive strain from 1.1-4 % were in the range of 5.7-8.0×10^{14} m^{-2}.

Introduction

GLIDCOP, dispersion-strengthened copper with ultra-fine particles of aluminum oxide, is used as a material for high-heat-load (HHL) components in many accelerator facilities due to its excellent thermal properties. In SPring-8 front ends, this material has been applied to many components such as masks, absorbers and XY slit assemblies, which are to be subjected to a maximum power density of approximately 1 kW mm^{-2} at a normal incidence for a standard in-vacuum undulator beamline. We investigated the thermal limitation of GlidCop under cyclic HHL conditions using specially designed GlidCop samples because of a progressive increase in the heat load from the insertion device [1]. As part of the investigation, the residual strain of the GlidCop samples was measured using synchrotron radiation and those results were almost in accordance with FEM analyses [2]. On the other hand, evaluation of the plastic strain, which was the main cause of fracture phenomena, was performed qualitatively by comparing the FWHM of the diffraction profiles of samples with unknown plastic strain, with that of samples with known plastic strain [3].

Recently, we investigated the plastic strain of HHL materials, including GlidCop, with regard to dislocation density, as the dislocation density generally correlates with the plastic strain. X-ray line profile analysis has been the most powerful method for investigating the dislocation structure in plastically deformed metal. In this study, we examined the dislocation density of GlidCop with compressive plastic strain loaded at high temperature, as the real components at SPring-8 frontend are subjected to compressive stress at high temperature. The modified Williamson-Hall and modified Warren-Averbach methods were applied to estimate the dislocation density [4].

Experimental

Two types of GlidCop samples, TP1 and TP2, were prepared. The grade of GlidCop used was AL-15. TP1, which was designed for low cycle fatigue fracture, was identical to those used in our previous studies [1,2]. It was comprised of an absorbing body made of GlidCop with a thickness of 2 mm, as well as a fitting cover and a cooling holder made of stainless steel. Before experiments with synchrotron radiation, cyclic heat loads were applied to the central area of TP1 samples using an

Materials Research Proceedings **2** (2016) 609-614 doi: http://dx.doi.org/10.21741/9781945291173-103

electron beam. The samples were subjected to 50 cycles and absorbed 550 W in each cycle; one cycle period comprised 7 minutes of thermal loading and 5 minutes of thermal unloading. The average maximum temperature of the TP1 samples was approximately 300 ºC during the heat cycles. The TP2 samples had known values of compressive strain. TP2 samples consisted of a cylinder with a diameter of 15 mm and a height of 15 mm. These samples were manufactured with compressive strains from 1.1-4 %. Compressive strains were applied at approximately 300 °C. After compression, the central volumes of TP2 samples, with a thickness of 2 mm, were cut by electrical discharge machining.

Profile measurements were performed using a transmission-type strain scanning method in the beamline of BL02B1 at SPring-8. Table 1 shows the experimental conditions used for the measurements. The measurements were carried out at the center of samples using Cu (111), (200), (311), (222), (400) and (331) reflections.

Table 1. Experimental conditions.

Beam line	SPring-8/BL02B1
Measurement method	Transmission-type strain scanning method
Energy [keV]	72.8
Monochromatic crystal	Si(311)
Diffraction and Diffraction angle (2θ) [°]	Cu(111): 4.67 Cu(200): 5.39 Cu(311): 8.95 Cu(222): 9.35 Cu(400):10.79 Cu(331):11.76
Slit size (Width × Height) [mm^2]	Divergent Slit 1: 2 × 0.2 Receiving Slit 1: 2× 2

Profile Analysis

The dislocation density was evaluated using the modified Williamson-Hall and modified Warren–Averbach methods, which are based on the FWHM value and the Fourier coefficient of the diffraction profile [4]. Assuming that line broadening is caused by dislocations, the modified Williamson-Hall method is expressed by the following equation:

$$\Delta K \cong 0.9/D + \sqrt{\pi M^2 b^2/2}\,\sqrt{\rho} K\sqrt{\bar{C}} + O(K^2\bar{C}), \quad (1)$$

where, $K = 2\sin\theta/\lambda$, ΔK is the FWHM, D is the average particle size, M is a constant, b is the absolute value of the Burgers vector, ρ is the dislocation density, $\bar{C}$ is the average contrast factor of the dislocations, and O indicates higher order terms in $K\sqrt{\bar{C}}$. Based on the theory of line broadening caused by dislocations, the average contrast factor in a cubic crystal system can be described as:

$$\bar{C} = \bar{C}_{h00}(1 - qH^2), \quad (2)$$

where $\overline{C}_{h00}$ is the average contrast factor corresponding to the (h00) reflection, q is a constant and $H^2 = \left(h^2k^2 + h^2l^2 + k^2l^2\right)/\left(h^2 + k^2 + l^2\right)$. Using Eq. 2, Eq. 1 can be expressed as:

Materials Research Proceedings **2** (2016) 609-614 doi: http://dx.doi.org/10.21741/9781945291173-103

$$((\Delta K)^2 - \alpha)/K^2 \cong \beta \bar{C}_{h00}(1 - qH^2), \quad (3)$$

where $\alpha = (0.9/D)^2$ and $\beta = \pi M^2 b^2 \rho/2$. From linear regression of the left hand side of Eq. 3 and H^2, the parameter q can be determined. The modified Warren–Averbach method can be described as follows:

$$\ln A(L) \cong \ln A^s(L) - (\pi b^2/2)\rho L^2 \ln(R_e/L)(K^2\bar{C}) + O(K^2\bar{C})^2, \quad (4)$$

where $A(L)$ is the real part of the cosine Fourier coefficient of the diffraction profile, A^s is the size Fourier coefficient, L is the Fourier length, and R_e is the effective outer cut off radius of dislocation and O represents higher order terms in $K^2\bar{C}$. By fitting the left hand side of Eq. 4 as a quadratic function of $K^2\bar{C}$, $A^s(L)$, the slope $X(L) = (\pi b^2/2)\rho L^2 \ln(R_e/L)$ can be obtained. The slope $X(L)$ can be evaluated according to the equation:

$$X(L)/L^2 = \rho(\pi b^2/2)(\ln R_e - \ln L). \quad (5)$$

From the linear regression of $X(L)/L^2$ and $\ln L$, the dislocation density, ρ, can be obtained.

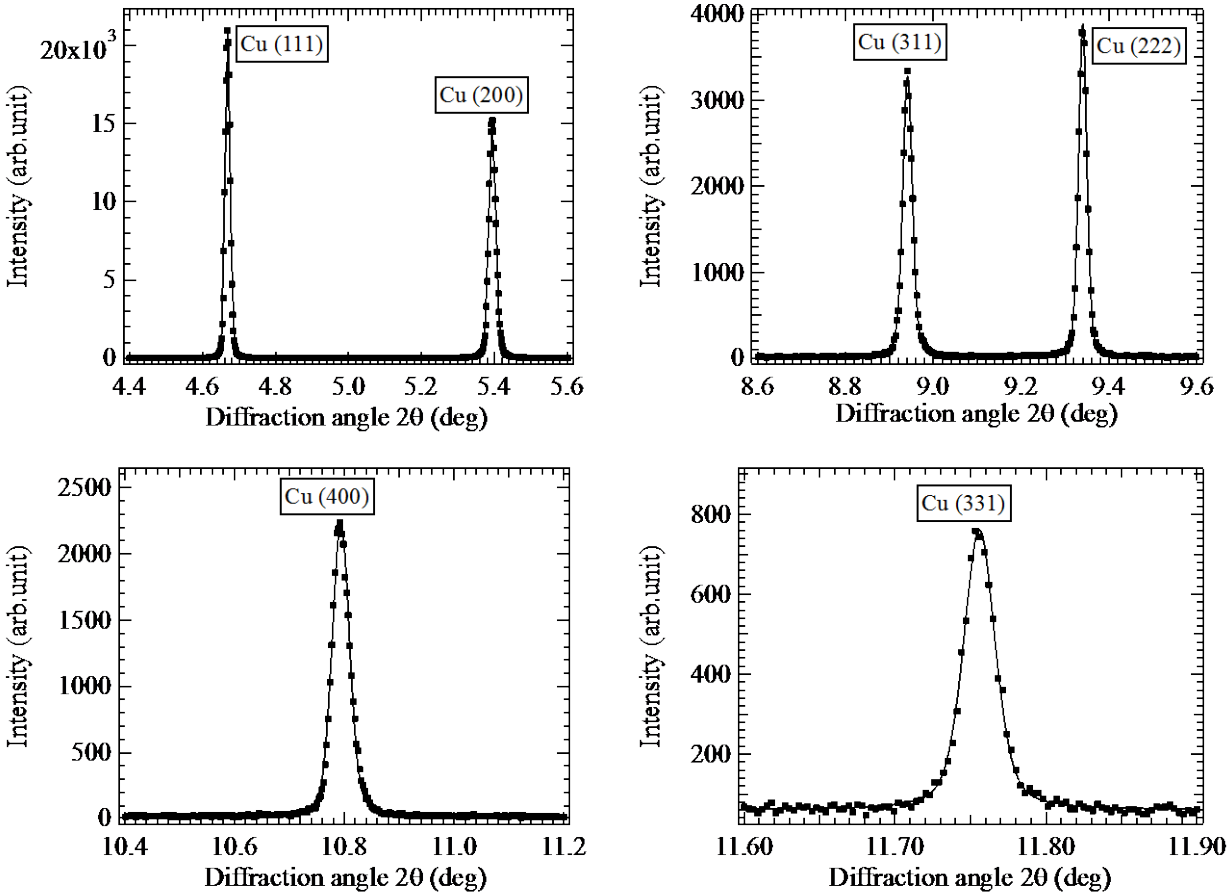

Figure 1: Cu(111), (200), (311), (222), (400) and (331) diffraction profiles of the TP2 sample under a compressive plastic strain of 1.6 %. The marks represent experimental data; the solid line corresponds to the fitting of a pseudo-Voigt function with a linear background.

Materials Research Proceedings **2** (2016) 609-614 doi: http://dx.doi.org/10.21741/9781945291173-103

Results

Fig. 1 shows the representative diffraction profiles for Cu (111), (200), (311), (222), (400) and (331) reflections of TP2 samples under a compressive plastic strain of 1.6 %. As shown in Fig. 1, a pseudo-Voigt function with a linear background was applied to the profiles as a fitting function. The FWHM and the real part of the cosine Fourier coefficients $A(L)$ were obtained from the fitting functions. In this study, it was assumed that instrumental line broadening was negligible, as the instrumental line broadening of the beamline was expected to be less than 0.002º, according to a previous study [5]. Fig. 2 shows the modified Williamson-Hall plots used to obtain q in the case of TP2 samples with compressive plastic strains of 1.6% and 3.3 %, respectively. The average contrast factor $\overline{C}_{h00}$ of copper adopted a value of 0.304 [6]. As shown in Fig. 3, using the Fourier coefficient of the profile, the modified Warren–Averbach method was applied to TP2 samples with compressive plastic strains of 1.6 % and 3.3 %. The value of slope $X(L)$ for each L value could be determined from the fitting of Eq. 4. The dislocation densities were evaluated from linear regression by Eq. 5, as shown in Fig. 4.

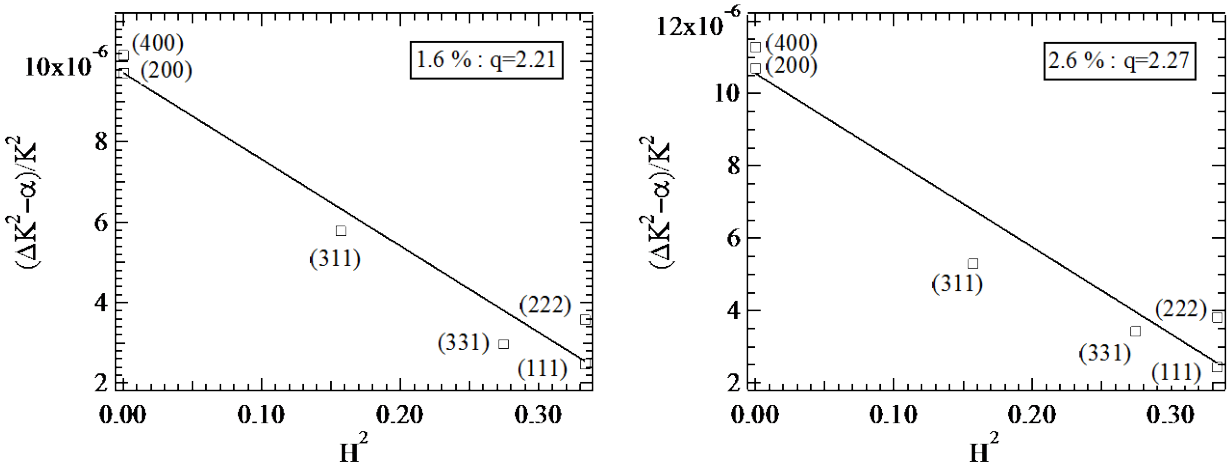

Figure 2: Relationship between $((\Delta K)^2 - \alpha)/K^2$ *and* H^2 *under compressive plastic strains of 1.6 % and 2.6 %. The solid line shows the fit of the data to Eq. 3.*

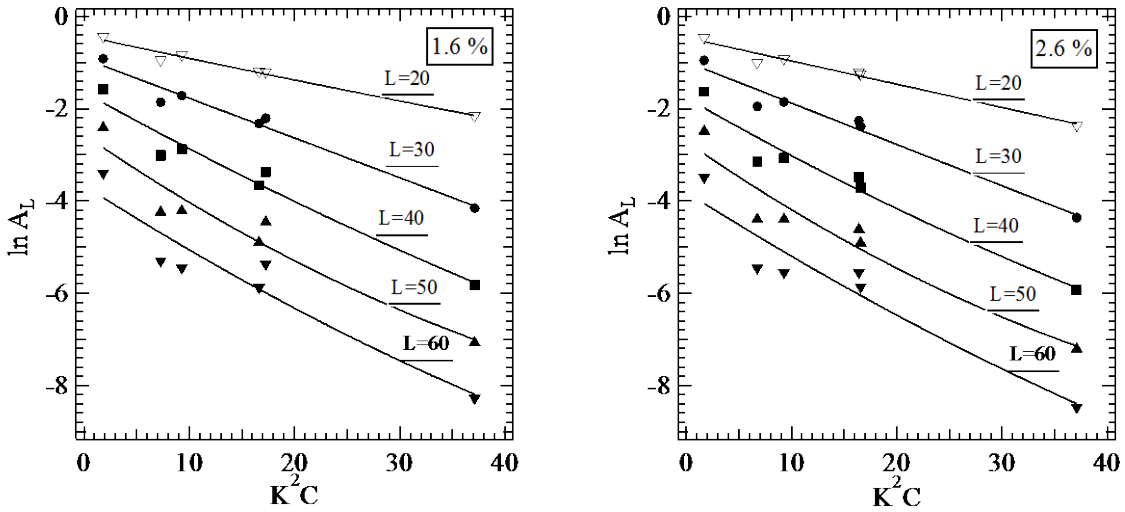

Figure 3: The relationship between $\ln A_L$ *and* K^2C *for each L value for compressive plastic strains of 1.6 % and 2.6 %. The solid line shows the fit of the data to Eq. 4.*

Materials Research Proceedings **2** (2016) 609-614 doi: http://dx.doi.org/10.21741/9781945291173-103

Fig. 5 shows *q*, the character of dislocation, for TP1 and TP2 samples, with theoretical values for each character of dislocation. The bottom and top axes show the compressive plastic strain for the TP2 samples and the number of cycles for the TP1 samples, respectively. While edge dislocation was predominant in the case of TP1 samples, for TP2 samples, screw dislocation was predominant within the range of measured compressive strains, and that character was close to pure screw dislocation with increasing compressive strain. Fig. 6 shows the dislocation densities of TP1 and TP2 samples. The dislocation density for TP2 samples gradually increased from 5.7×10^{14} m^{-2} to 8.0×10^{14} m^{-2} with increasing compressive strain. On the other hand, the dislocation density of TP1 sample after 50 cycles was 5.7×10^{14} m^{-2}.

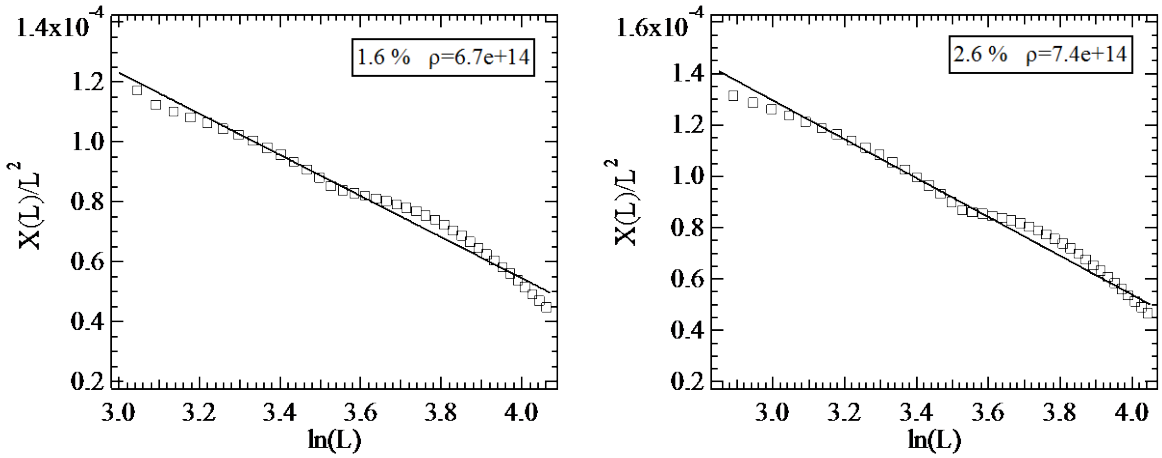

Figure 4: Relationship between $\boldsymbol{X(L)/L^2}$ *and* $\boldsymbol{\ln L}$ *for compressive plastic strains of 1.6 % and 2.6 %. The solid line shows the fit of the data to Eq. 5.*

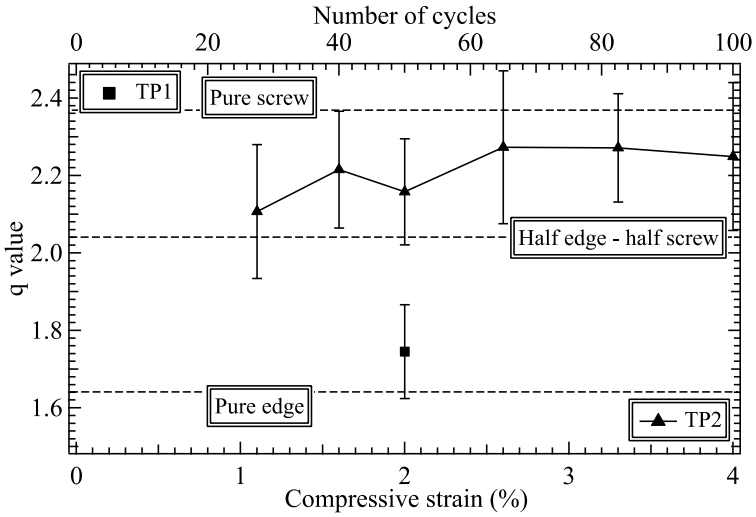

Figure 5: Relationship between the compressive strains of TP2 samples, the number of cycles of TP1 samples and q. The horizontal dotted lines show the theoretical values for each character of dislocation.

Summary

We estimated the dislocation densities of GlidCop samples with compressive strains at high temperature using X-ray diffraction profiles by applying the modified Williamson-Hall and modified

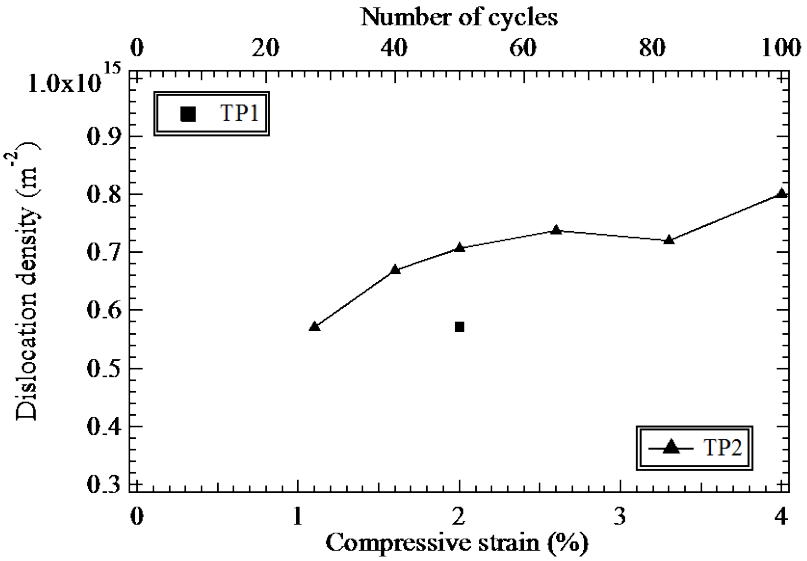

Figure 6: Relationship between the compressive strain of TP2 samples, the number of cycles of TP1 samples and dislocation density.

Warren-Averbach methods. The dislocation densities of TP2 samples gradually increased with increasing compressive strain, while that of TP1 samples was close to the value of TP2 samples with 1.1 % compressive strain.

Acknowledgement
The synchrotron radiation experiments were performed at the SPring-8 with the approval of the Japan Synchrotron Radiation Research Institute (JASRI) (Proposal No. 2014B1412).

References

[1] S. Takahashi, M. Sano, T. Mochizuki, A. Watanabe, H. Kitamura, Fatigue life prediction for high-heat-load components made of GlidCop by elastic-plastic analysis, J. Synchrotron Rad. 15 (2008) 144-150. https://doi.org/10.1107/S090904950706565X

[2] M. Sano, S. Takahashi, A. Watanabe, H. Kitamura, K. Kiriyama, T. Shobu, Internal residual strain of GlidCop for materials of the high-heat-load components, Materials Science Forum, 652 (2010) 222-226. https://doi.org/10.4028/www.scientific.net/MSF.652.222

[3] M. Sano, S. Takahashi, A. Watanabe, H. Kitamura, S. Shiro, T. Shobu, Plastic strain of GlidCop for materials of high heat load components, Materials Science Forum, 772 (2014) 123-127. https://doi.org/10.4028/www.scientific.net/MSF.772.123

[4] T. Ungar, A. Borbely, The effect of dislocation contrast on x-ray line broadening: A new approach to line profile analysis, Appl. Phys. Lett. 69 (1996) 3173-3175. https://doi.org/10.1063/1.117951

[5] Y. Noda, Current Status of Crystal Structure Analysis BL02B1 Experimental Station, SPring-8 INFORMATION, Volume 02, No.5 (1997) 17-23.

[6] T. Ungar, I. Dragomir, A. Revesz, A. Borbely, The contrast factors of dislocations in cubic crystals: the dislocation model of strain anisotropy in practice, J. Appl. Cryst. 32 (1999) 992-1002. https://doi.org/10.1107/S0021889899009334